frontiers | Frontiers in Earth Science

ORIGINAL RESEARCH
published: 01 July 2022
doi: 10.3389/feart.2022.909102

Experimental Analysis on Mechanical Characteristics of Foundation Soil in Rift Valley Area of Kenya Nairobi-Malaba Railway

Bing Hao[1], *Zhenghua Zhou*[1], *Yuandong Li*[1], *Xiaojun Li*[2]* and *Liguo Jin*[3]

[1]College of Transportation Engineering, Nanjing Tech University, Nanjing, China, [2]Key Laboratory of Urban Security and Disaster Engineering of China Ministry of Education, Beijing University of Technology, Beijing, China, [3]Institute of Geophysics, China Earthquake Administration, Beijing, China

The Rift Valley section of Kenya Nairobi-Malaba Railway locates in the Great Rift Valley of East Africa, with complex engineering geological conditions and well-developed geological structures. During the rainy season from March to May 2018, four large-scale ground fissures were formed in the first-stage project of the Nairobi-Malaba Railway of the valley floor section, accompanied by uneven surface settlement and trenches, seriously endangering the safety of the railway and its nearby projects. Through field investigation, it is preliminarily considered that the main reason induced ground fissures and surface settlement is the underlying soil layer being eroded by groundwater. The gully is further formed by surface water erosion on a base of uneven surface subsidence. The geological exploration trench at DK77 ground fissure revealed that the overlying soil layer is respectively grayish-yellow silty clay, cyan-gray volcanic ash, and brownish-yellow silty clay from top to bottom, and the underlying bedrock is volcanic tuff with wide cracks. The fluid flows out or into the bedrock through the cracks developing channels for groundwater up-down flowage. Under the erosion of groundwater to the underlying soil, this study proved the possibility of the occurrence of uneven settlement. When exposed to the groundwater, the underlying soil will exhibit special physical and mechanical properties which are conducive to the occurrence of ground cracks and subsidence. The conventional geotechnical tests are conducted for the three types of overlying soil, and the results reveal the causes of ground fissures and surface settlement from the physical and mechanical properties of the overlying soil and provide a basis for the further qualitative analysis of the mechanism of ground fissures and surface settlement.

Keywords: ground fissure, uneven settlement, collapsibility, subsurface erosion, clay content

OPEN ACCESS

Edited by:
Guang-Liang Feng,
Institute of Rock and Soil Mechanics (CAS), China

Reviewed by:
Liyuan Tong,
Southeast University, China
Wenjun Zheng,
Sun Yat-sen University, China
Meigen Zhang,
Institute of Geology and Geophysics (CAS), China

***Correspondence:**
Xiaojun Li
lixiaojun@bjut.edu.cn

Specialty section:
This article was submitted to Geohazards and Georisks, a section of the journal Frontiers in Earth Science

Received: *31 March 2022*
Accepted: *23 May 2022*
Published: *01 July 2022*

Citation:
Hao B, Zhou Z, Li Y, Li X and Jin L (2022) Experimental Analysis on Mechanical Characteristics of Foundation Soil in Rift Valley Area of Kenya Nairobi-Malaba Railway. Front. Earth Sci. 10:909102. doi: 10.3389/feart.2022.909102

1 INTRODUCTION

During the rainy season from March to May 2018, four large-scale ground fissures were generated in the East African Rift Valley section of the first phase of the Nairobi-Malaba Railway Project, accompanied by multiple uneven surface settlements, which seriously endangered the safety of the railway and its nearby projects. Considering that the safety of the Nairobi-Malaba Railway is related to the sustainability of the national, it is of great significance to deeply study these ground fissures to ensure the safe construction and operation of the Nairobi-Malaba Railway.

Ground fissure with a certain length and width on the ground is a macroscopic geological destruction phenomenon in which surface rock and soil crack under the action of natural or human factors (Youssef, 2013). As a geological disaster, ground fissures have caused serious harm to the natural environment and human engineering activities. Since Leonard (1929) devoted himself to the study the ground fissures in 1929 at first, subsequently a few scholars have studied the ground fissures, mainly focusing on the genetic mechanism, regularity of spatial distribution, and activity characteristics of ground fissures. The genetic mechanism involves geological tectonic activities (Ayalew, et al., 2004; Sarkar, 2004; Conway, 2015; Xu et al., 2016), underground mining (Budhu, 2011; Gabrielli et al., 2011; Youssef et al., 2014; Jin et al., 2016; Feng, et al., 2022), underground erosion of loess (Liu et al., 2015; Peng et al., 2020; Leng et al., 2021), and other factors (Fergason et al., 2015; Elahe et al., 2020; Jia et al., 2020). The regularity of spatial distribution shows that the overall trend of the ground fissures is approximately the same as that of the regional fault structures (Wang et al., 2020). The ground fissures with a large width in the ancient river course site, the artificial backfill soil site, and the low-lying and underwater mining settlement site have many branches (Nina et al., 2019). The activity characteristics show three-dimensional movement characteristics, that vertical movement, horizontal movement, and the movement rate of vertical movement are the largest while that of horizontal movement is relatively small (Timothy et al., 2016; Howard and Zhou, 2019; Liu et al., 2019). In recent years, with the massive construction of various infrastructure facilities under complex site conditions, the impact of ground fissures on the project has become increasingly prominent.

Among the four ground fissures formed in the Rift Valley area, DK76, DK77, and B3 road fissures are large in scale. Combined with previous studies on ground fissures, B3 road fissures have the characteristics of typical fault-type ground fissures, while the others show the phenomena of the discontinuous gullies, holes of different sizes in shallow soil, and uneven settlement of local surface, which are obviously different from fault-type ground fissures, and its genesis is difficult to be inferred. Our research aims to deeply study the genesis of ground fissures and surface subsidence in the rift zone, to provide a basis for the prevention and control of ground fissures and surface subsidence in railway projects and nearby constructions.

The research is divided into four stages: the first stage is to analyze the characteristics of undisturbed soil through basic physical properties experiments; the second stage is to analyze the influence of water content on the physical and mechanical properties of the soil, considering that ground fissures occur in the rainy season; next, put forward the hypothesis of ground fissure mechanism and the last, set up a series of simulation physical model experiments and give quantitative results to verify the hypothesis. This article presents the research results of the first three stages, and the results of the fourth part will be presented in the subsequent contents.

2 SUMMARY OF GROUND FISSURE AND SURFACE SUBSIDENCE IN RIFT VALLEY AREA

Since March 2018, four ground fissures have appeared successively in the Kenya Nairobi-Malaba Railway rift region (Geographical distribution is presented in **Figure 1**). Among them, the three large-scale ground fissures are respectively named B3 highway ground fissure, DK76 ground fissure, and DK77 ground fissure.

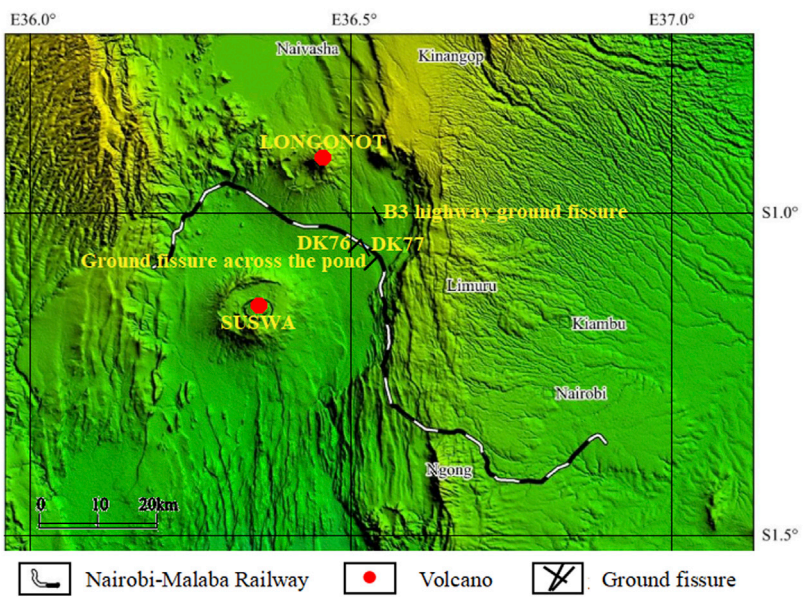

FIGURE 1 | Geographical distribution map of the fissures.

FIGURE 2 | Scene photos of ground fissures near the railway. **(A)** DK76; **(B)** B3 highway; **(C)** DK77; **(D)** ground fissure through a pond.

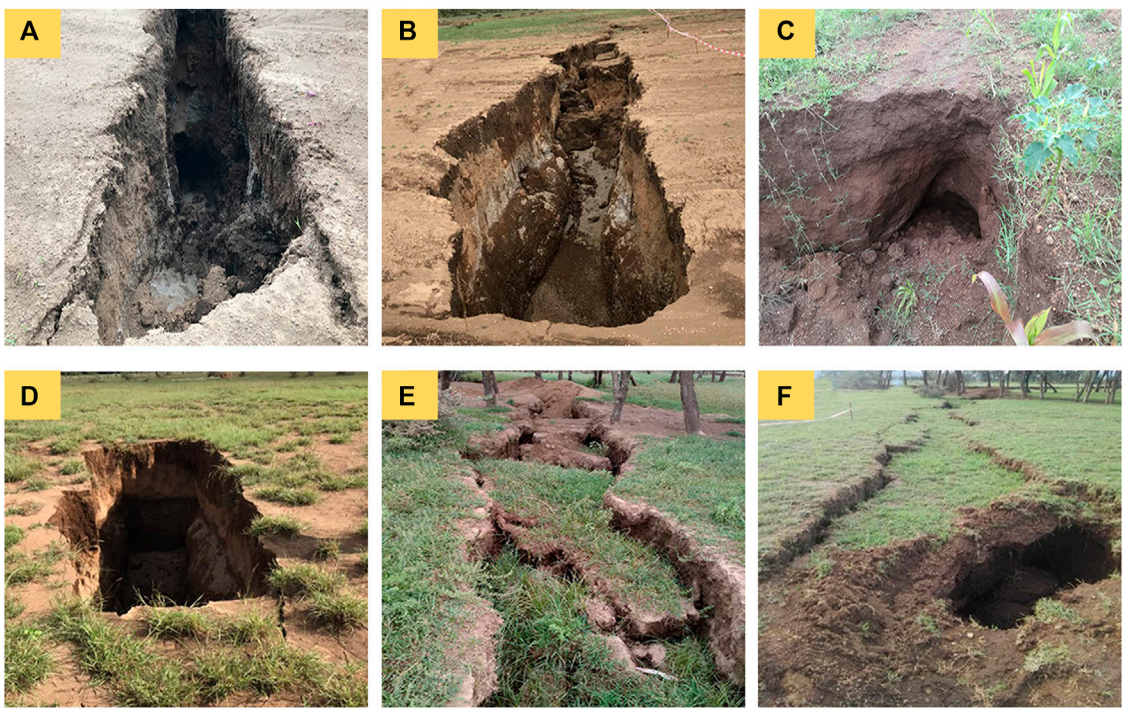

FIGURE 3 | Ground fissure morphology along the railway. **(A, B)** Discontinuous gullies; **(C, D)** holes of different sizes; **(E, F)** uneven settlement.

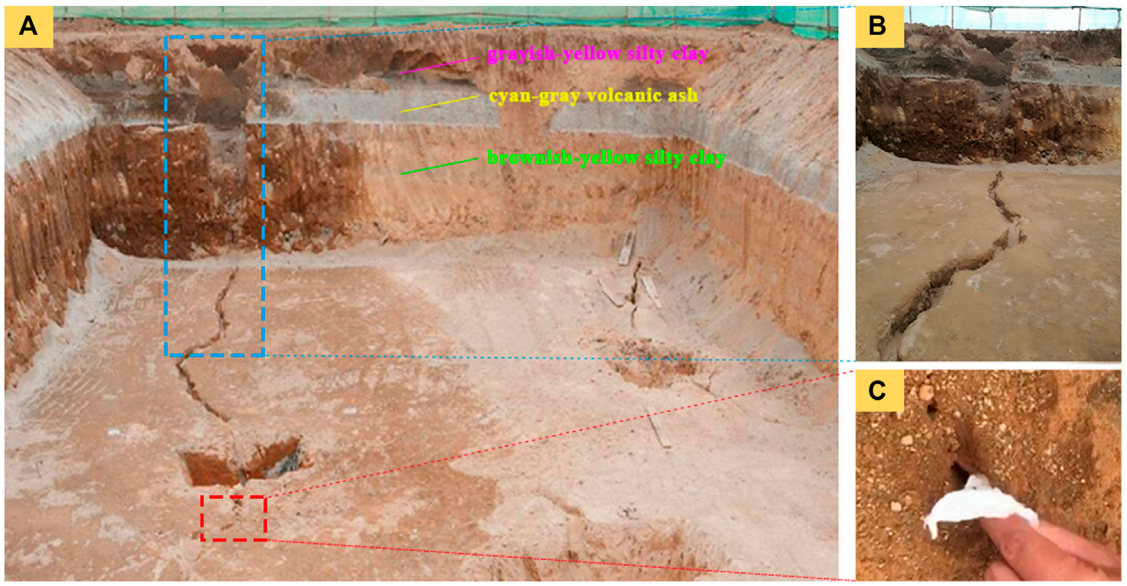

FIGURE 4 | Geological section and details of exploration trench. **(A)** The trench scene; **(B)** collapse and the crack facing it; **(C)** a small hole with air friction sound.

Due to consecutive rainfall, a ground crack and gully nearly orthogonal to the line appeared at DK76 + 798 of the Nairobi-Malaba Railway on 7 March 2018. the ground crack started at 50.0 m on the left side of the line, ran from north to south, gradually widened toward the right side of the line, and formed a gully, crossing the front channel, the gully was 3.4 m deep, 0.5–1.5 m wide and about 200.0 m long (as shown in **Figure 2A**). The ground fissure of the B3 highway is located near Nakuru in the Rift Valley region of East Africa, after several days of continuous rainfall, the ground fissure suddenly occurred and formed gullies on the evening of 13 March 2018, the ground fissure runs from north to south with a depth of 15 m, a width of 2–5 m, a length of several kilometers and cuts off B3 highway, according to the description of witnesses at the scene of the accident, the ground fissure occurred suddenly and developed rapidly (**Figure 2B**). The DK77 ground fissure is located at DK77 + 884 of the Nairobi-Malaba railway, 1 h after heavy rainfall on 4 May 2018, a crack with a north–south strike, a depth of 2–5 m, a width of 1–2 m, and a length of 300 m appeared (**Figure 2C**). The fourth ground fissure passes through a pond and intersects with the branch line of Nakuru-Kiambu Highway, which is approximately parallel to the south and north of the B3 Highway fissure, but with a smaller scale (**Figure 2D**).

According to geological mapping, the B3 highway ground fissure is a series of normal faults along the eastern boundary fault zone of the East African Great Rift Valley. Its strike is nearly the north–south direction, consistent with the strike of the fault, straight line, stretching for several kilometers, and continuous through, with a width of 2–5 m, which is a typical fault type ground fissure. While ground fissure of DK76, DK77, and the one through a pond is not only relatively short in length but also have discontinuous gullies (as shown in **Figures 3A**, **B**), holes of different sizes exist in shallow soil (**Figures 3C**, **D**), with uneven settlement occurs on the local surface (**Figures 3E**, **F**). The above characteristics of ground fissures indicate that the ground fissures and uneven surface settlement are not caused by earthquakes or surface rain erosion, but by the underlying soil layer being eroded by groundwater, while gullies are formed by surface water erosion based on uneven surface settlement. The existence of holes of different sizes in the shallow soil further supports this conjecture. At the same time, the surface vegetation at the uneven settlement of the surface is complete, which also indicates that the formation of ground fissures is related to the loss of the underlying soil mass.

To verify the above conjecture and investigate whether the underlying soil layer is disturbed and whether fissures are developed in the underlying bedrock, a geological trench survey was carried out at DK76 and DK77 (as shown in **Figure 4A**). The trench excavation shows that the left and right bedrock cracks are visible in the weathered layer of bedrock. The strike of the cracks on the right side of the trench is consistent with the surface cracks. The underground cracks are exposed to the overlying soil layer with settlement and collapse, and the discontinuity caused by collapse can be observed in the volcanic ash layer. The crack on the left side of the exploration trench is exposed to the new crack position, and there is an obvious collapse phenomenon at the overlying soil layer where the underground crack is facing directly (**Figure 4B**). The volcanic ash layer is interrupted due to the collapse of the soil layer; thus, it can be seen that the collapse of the soil layer is related to the underground bedrock crack. Meanwhile, fluid overflow was observed at the crack at the bottom of the trench, accompanied by a slight air friction sound, that is, there was the internal and external exchange of gas, which proved that there was a channel for fluid flow under the bedrock crack (**Figure 4C**).

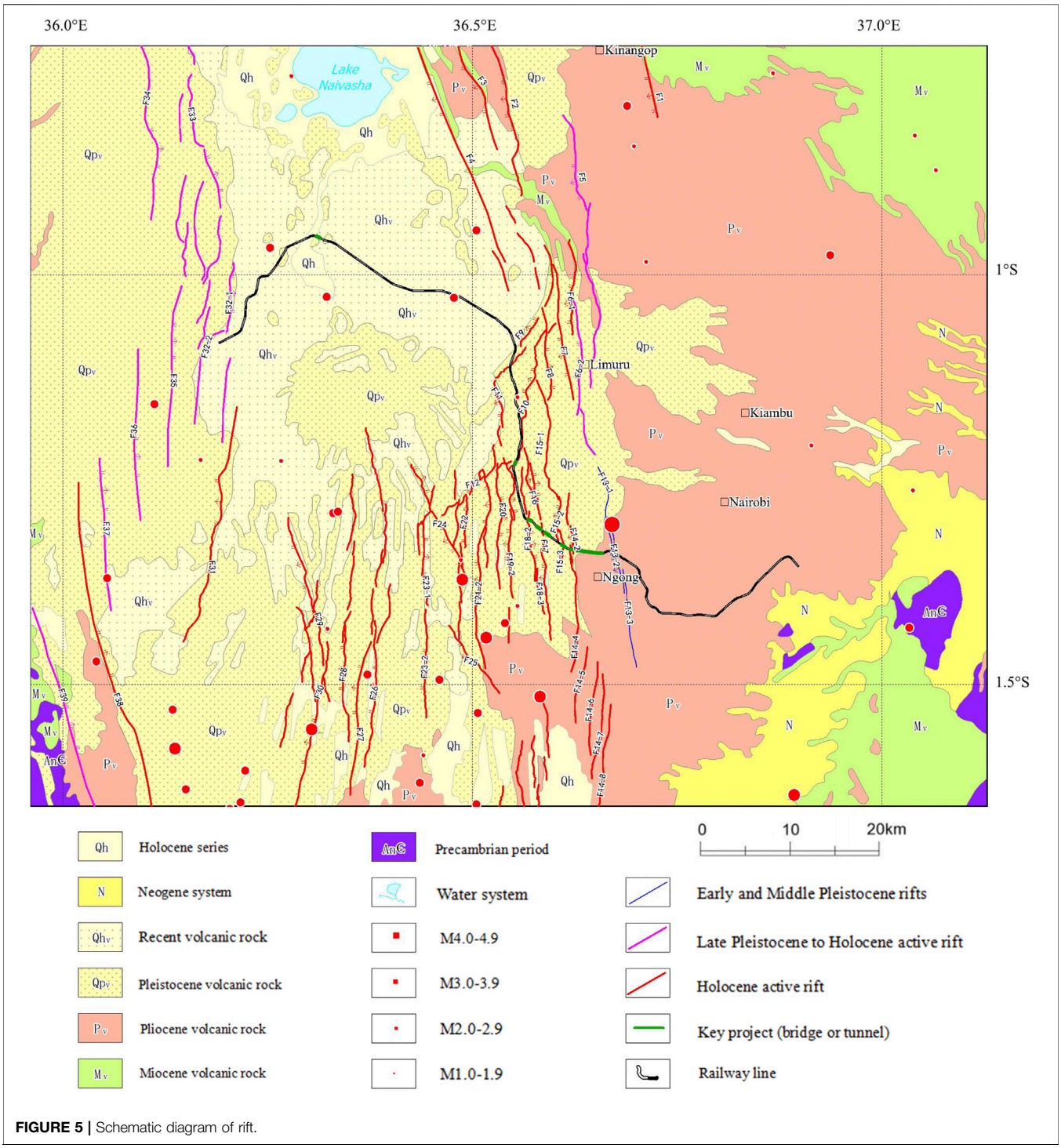

FIGURE 5 | Schematic diagram of rift.

Based on the results of the exploration trench, it is speculated that after continuous rainfall infiltration in the rainy season, a part of soil particles in the overburden migrate downward and lose along the bedrock cracks. At the same time, soil particles near the rock-soil interface are continuously lost along the bedrock cracks and gradually form holes under the action of underground water erosion. When the holes develop to a certain scale, it collapses unsteadily due to rainfall inducement, and the surface first appears one by one pit. With the continuous development and connection of the pits, the collapse forms ground fissures and uneven settlement of the surface, then scoured by surface rainwater to form gullies.

3 ENGINEERING GEOLOGICAL CONDITIONS OF SURFACE FISSURE SITE

3.1 Site Construction Environment

The first phase of the Nairobi-Malaba railway project in Kenya starts from Nairobi, Kenya's capital, and ends near Narok. The line passes through the floor area of the Great Rift Valley in East Africa. The valley floor area is about 40 km wide, with open and flat terrain, lava platforms, huge volcanic cones, and cliffs on both sides. The height difference between the valley floor and the top of the cliff is 450–2,000 m, and the ground elevation of the valley floor area is 1,650–1,820 m (Wang et al., 2019).

The valley floor area is a fault depression zone of the Great Rift Valley across North and South Africa, the geological structure is well developed, and most of the faults are Holocene active faults. The traces of these faults to the north are mostly covered by newer pyroclastic rocks and volcanic ash, with almost no outcrop on the surface. According to the comprehensive geophysical exploration results, there are 16 concealed rift fracture zones distributed under the overburden (**Figure 5**). In addition, a series of volcanoes are distributed in the Rift Valley area, mainly the SUSWA volcano on the south side of the line and the LONGONOT on the north side (Wadge et al., 2016), their distribution is shown in **Figure 1**. The floor area of the East African Rift Valley traversed by the line is characterized by active geological structure, frequent volcanoes, and geothermal anomalies, which provide basement structural conditions for the generation and development of underlying bedrock cracks.

3.2 Geotechnical Engineering Geological Characteristics

The overlying soil in the valley floor area is mainly Quaternary Holocene-Pleistocene strata. The overlying soil of pyroclastic accumulation and diluvium layer is stratified mainly composed of silty clay, volcanic ash, etc., with the characteristics of a large pore ratio, loose structure, poor gradation, and strong water permeability. The underlying bedrock is mainly volcanic tuff, covering the semi-diagenetic strata in the early Tertiary and Quaternary. The rock is hard and has concealed structural fractures, with tensile fractures and cavities distributed, which become channels for groundwater to flow up and down.

According to the engineering geological exploration report near the DK76 ground fissure, it can be seen that the engineering geological characteristics of the geotechnical layer exposed by the exploration trench are as follows: 1) silty clay: grayish-yellow, hard plastic, with high silty content and relatively uniform soil texture; 2) volcanic ash: cyan-gray, slightly wet, slightly dense, flaky particles, containing a small amount of gravel, accounting for 5%–10%, with poor gradation; 3) silty clay: brownish-yellow, hard plastic, mixed with fine sand, with high silty content; 4) tuff: brownish-gray, tuff structure, and blocky structure; drill core is 8–40 cm in a short column shape, locally broken blocky, with dumb hammering sound and easy to break. Under the geological background of the valley floor area where the line is located, combined with the above investigation and engineering geological investigation, it is qualitatively believed that the Rift Valley area has engineering geological and hydrogeological conditions for the development of ground fissures, and it is inferred that the ground fissures are the result of suffosion erosion effect of groundwater on the overlying soil layer through underlying bedrock cracks. The underlying bedrock crack is the prerequisite for the formation of the ground fissure, which determines the nature and spatial distribution characteristics of the ground fissure.

Considering that the main overlying soil layers may exhibit unique physical and mechanical properties when mixing with water, which are extremely vulnerable to groundwater erosion, causing structural damage or being washed away, thus resulting in ground fissures and surface settlement. Therefore, conventional geotechnical tests are carried out on the grayish-yellow silty clay, cyan-gray volcanic ash, and brownish-yellow silty clay samples obtained from drilling, to reveal the causes of ground fissures and surface settlement from the physical and mechanical properties, to provide a basis for their prevention and control.

4 TEST AND ANALYSIS OF SOIL MECHANICS AND PHYSICAL CHARACTERISTICS

4.1 Basic Physical Indexes of Soil and Analysis

According to the basic requirements of the geotechnical test, combined with the purpose of this test, dry density, specific gravity, water content, plastic limit, liquid limit, and porosity are selected as the basic physical indexes of the three types of soil to be measured. Specific gravity is measured by the pycnometer method, water content is measured by the drying method, plastic, and liquid limits are measured by plastic-liquid limit combined tester, and porosity is obtained by conversion of specific gravity, water content, and density according to the corresponding engineering geological exploration report which is based on Rules of Geotechnical Testing (GB/T50123-2019). The detailed experimental results are listed in **Table 1**.

According to the test results, the specific gravity and plastic and liquid limit indexes of the three types of soils are not significantly different from the similar soils of other regions. However, there were obvious differences in the state of the three types of soils after water immersion: after drying the grayish-yellow silty clay, the surface layer of the soil has a liquid-like touch (as shown in **Figure 6A**), which proves that it has a finer particle size. In addition, when it is sieved with 0.075 mm particle size, most of the particles will be sieved, but during the sieving process, a layer of soil film formed by interlinking fine particles tended to form on the surface layer of the sieve, which hinders the particles from passing through the sieve. This phenomenon indicates that this type of soil has a strong cementation effect at a lower water content, so it may have strong collapsibility. At 10% water content, the brown color deepens, and the fine particles form small balls, which crumble into powdered particles when lightly touched (**Figure 6B**). Under 20% water content, the brown color is deeper, the strength of the small balls formed with water

TABLE 1 | Basic physical indexes of three types of soils.

Types of soil	Dry density (g/cm^3)	Water content (%)	Specific gravity	Plastic limit (%)	Liquid limit (%)	Porosity
Grayish-yellow silty clay	1.31	17.82	2.71	15.31	34.29	0.58
Cyan-gray volcanic ash	1.42	10.07	2.68	19.57	38.71	0.52
Brownish-yellow silty clay	1.33	13.15	2.70	16.19	37.25	0.56

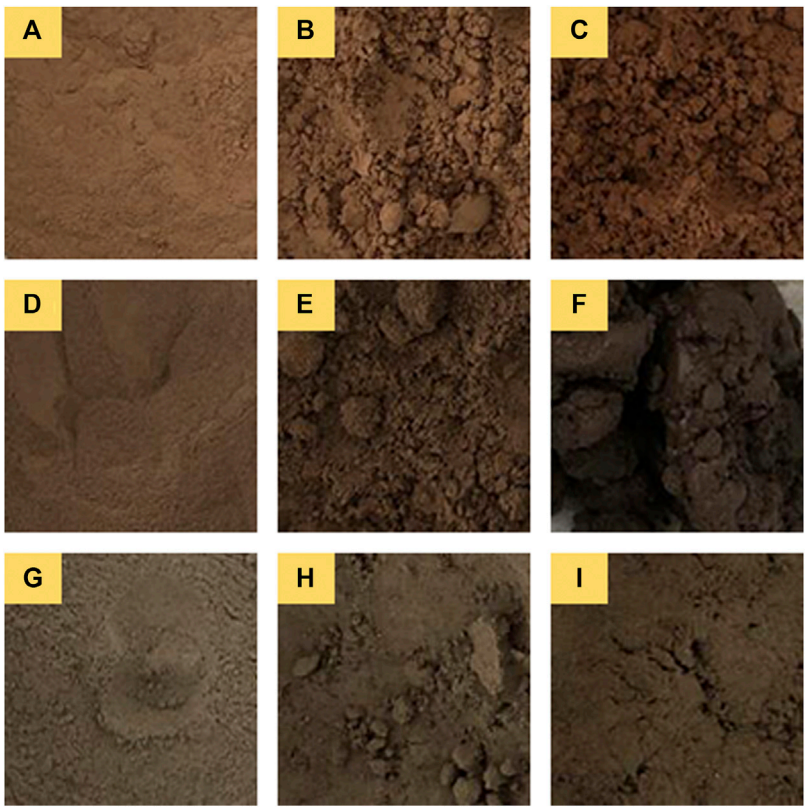

FIGURE 6 | Apparent phenomena of three kinds of experimental soils at different water contents. **(A)** Dried grayish-yellow silty clay; **(B)** 10% water content grayish-yellow silty clay; **(C)** 20% water content grayish-yellow silty clay; **(D)** Dried brownish-yellow silty clay; **(E)** 10% water content brownish-yellow silty clay; **(F)** 20% water content brownish-yellow silty clay; **(G)** Dried cyan-gray volcanic ash; **(H)** l0% water content cyan-gray volcanic ash; **(I)** 20% water content cyan-gray volcanic ash.

increases slightly, which crumble into powdered particles when lightly touched too (**Figure 6C**); the brownish-yellow silty clay is dry to the touch, and the connection between particles is weak, so there is no sieving conjunctive phenomenon (**Figure 6D**). At 10% water content, fine particles are combined into small balls with water, form smaller balls when pinched but do not crumble into powdered particles (**Figure 6E**), and at 20% water content, the brown color is darker, the small balls with water have higher strength, higher soil plasticity, not easy to be pinched, with high viscosity (**Figure 6F**). After drying, the cyan-gray volcanic ash is dry to the touch, with a weak connection between fine particles and no sieving conjunctive phenomenon (**Figure 6G**). Under 10% water content, the particles are knitted into larger clods, but the connection between particles is weak, and they are broken into multiple clods when lightly touched (**Figure 6H**); at 20% water content, the color deepens, the soil particles are connected to form larger clods, and the connection force between particles is still weak (**Figure 6I**).

Combined with the apparent phenomena of three kinds of soils with different water contents and the fact that ground fissures and uneven settlement occurred after several heavy rainfalls, it is inferred that the water content has an important influence on the mechanical properties of soil, and the clay content in the soil which is easy to be scoured by water may also be the cause of the occurrence of ground fissures. Therefore, the following experiments are carried out from three aspects, respectively, the direct shear experiment at different water contents to determine the effect of water content on the strength of the soil, the collapsibility test to determine the extent of collapsibility in a saturated state, and the clay content experiment to determine the proportion of clay particles in the fine particle soil. In the following, we first

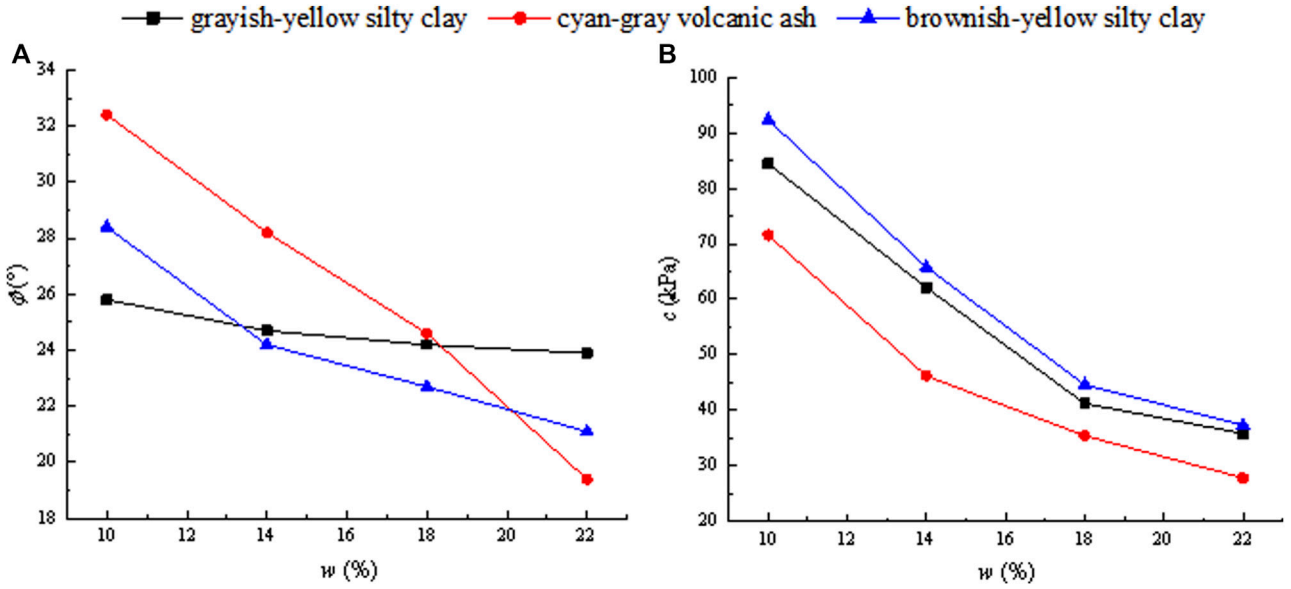

FIGURE 7 | Results of the direct shear test. **(A)** Relationship between cohesion and water content; **(B)** relationship between internal friction angle and water content.

analyze the variation characteristics of mechanical properties of the above three types of soils under the condition of different water contents.

4.2 Direct Shear Test

To study the influence of soil moisture content on its shear strength, three types of soil with water contents of 10%, 14%, 18%, and 22% were selected for direct shear tests, and the relationship between cohesion and internal friction angle with water content as represented in **Figure 7**. It can be observed that the cohesion and internal friction angle of the three types of soils decrease with the increase of water content. The cohesive force of brownish-yellow silty clay and grayish-yellow silty clay under different water contents are close to each other, and both are greater than that of cyan-gray volcanic ash, and the cohesive force decreases faster with the increase of water contents. The internal friction angle of the three types of soils shows obvious differences with the change in water content. The internal friction angle of the cyan-gray volcanic ash decreases rapidly with the increase of water content. The internal friction angle of the brownish-yellow silty clay decreases rapidly with the increase of water content at lower water content. When the water content is higher than 14%, the decreased speed of the internal friction angle becomes slower. The internal friction angle of grayish-yellow silty clay decreases slightly with the increase of water content.

4.3 Collapsibility Test

4.3.1 Test Preparation

From the above tests, it can be obtained that the moisture content has a significant impact on the shear strength of the three soils. Based on the different apparent characteristics of the three types of soil when meeting water in the sample preparation process, we will conduct collapsibility tests to quantitatively analyze the influence of the water immersion process on the mechanical properties of these soils. The main influencing factors of collapsibility include soil structure, overlying pressure, and water content,. Soil structure is affected by deposition conditions, mainly manifested by the degree of cementation between particles and the number of unstable macropores; overburden pressure is mainly controlled by the depth of the soil layer; water content is related to the strength of cementation before collapsibility, capillary pressure, matric suction, and soil permeability.

In the process of sampling, the three undisturbed soil samples in this test are all in a fragmented state after being taken out, which indicates that the soil structure generated by the natural deposition process is weak, and the soil structure loss is caused by remolding process is relatively small. For two soils with the same size and pore ratio, the bearing capacity of remolded soil will be larger than that of undisturbed soil; that is, remolded soil shows stronger collapsibility, so it is more conservative to calculate the settlement based on the results of remolded soil.

Based on the above factors, the collapsibility tests were conducted for three soils with axial pressure of 200 kPa, a porosity of 0.55, and water content of 5, 10, 13, 15, 17, and 20%, respectively.

4.3.2 Test Results and Analysis

The collapsibility test results of the three types of soil are shown in **Figure 8**. The collapsibility of the three types of soil will be analyzed based on the test results.

4.3.2.1 Grayish-Yellow Silty Clay

The collapsibility test results show that the collapsibility coefficient of grayish-yellow silty clay is very low, and its collapsibility gradually loses with the increase of water content. Combining the apparent phenomena in the sample preparation

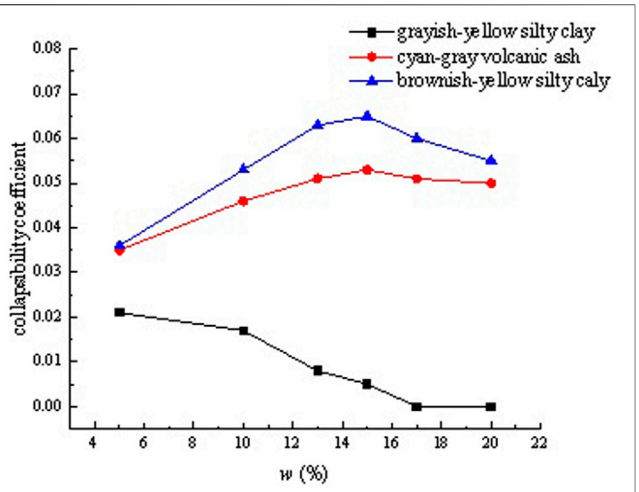

FIGURE 8 | Variation of collapsibility coefficient with water content.

process, the reasons for the variation of collapsibility coefficient under different water contents are analyzed: When the soil with lower water content starts to infiltrate, soil particles form small balls that are not easy to crush, and the combination between the particles becomes tight, soil structure gradually strengthens, and the macroscopic manifestation is that a small amount of settlement occurs in the soil. When water infiltrates to a certain extent, soil structure reaches the strongest, the formed particles are high in strength and viscosity, similar to plasticine, and will not be damaged due to further flooding, and the settlement will not increase in macroscopic.

For the soil with higher water content, the structure obtained by the preparation process is stronger than that with lower water content, and the settlement generated during infiltration is small; that is, collapsibility is small. When water content reaches 17%, the sample will no longer become compact due to immersion. At the same time, it will not cause structural damage due to the high strength and viscosity of the particles. Macroscopically, the settlement is zero, that is, there is no collapsibility.

4.3.2.2 Cyan-Gray Volcanic Ash

The test results show that the collapsibility coefficient of cyan-gray volcanic ash is relatively high, and the collapsibility increases to an extreme value first and then decreases slowly with the increase of water content, the test results are analyzed as follows: Volcanic ash particles have a poor affinity for water. Under low water content, the particles are arranged in a neat and tuff structure, which has strong structural properties. After encountering water, the tuff structure is partially destroyed, showing certain collapsibility. At higher water content, the surface of the sample shows a bleeding phenomenon, the arrangement of volcanic ash is scattered, and no tuff structure formed. The structure is obviously destroyed and collapsibility is significantly increased after mixing with water. When the water content continues to increase, the bleeding phenomenon on the surface of the sample is more obvious, and the structural property of volcanic ash is very weak, thus reducing the structural damage caused by collapsibility and reducing the collapsibility coefficient.

4.3.2.3 Brownish-Yellow Silty Clay

The test results show that brownish-yellow silty clay has the strongest collapsibility under each set of water content, which also has a process of first increasing and then decreasing with the increase of water content. In the screening process of sample preparation, it is found that brownish-yellow silty clay has an obvious "conjunctiva" phenomenon. Even when dry soil passes through a 0.075 mm sieve, fine particles that can be sieved will form a dense soil film on the surface of the sieve, which hinders the sieving of particles. When the sieve is knocked, the soil film is damaged and fine particles are sieved. It shows that the cohesive force of this kind of soil is strong under low water content. when the soil with low water content begins to soak, soil particles form small balls, the combination between the particles becomes tight, soil structure gradually increases, and the macroscopic manifestation is a small settlement. When the soil soaks to a certain extent, its structure will damage, and the settlement amount will further increase; when the soil with higher water content begins to infiltrate, the structure of the sample itself is stronger than that with lower water content, the structural damage and settlement are large; that is, collapsibility is strong. When the water content of the sample is very high, the structure of the soil becomes weak, the structural damage in the infiltration process is small, the settlement amount is small, and the collapsibility is weakened.

In addition, combining the exploration trench and drilling data, brownish-yellow silty clay is located on the underlying bedrock tuff, which is easily eroded by groundwater. Its properties are important factors that affect the ground settlement.

4.3.3 Analysis on Influencing Factors of Collapsibility

According to collapsibility theory, collapsibility is not only affected by soil structure and water content, but also by overlying pressure. In the following, the collapsibility tests on strong collapsibility soils of brownish-yellow silty clay and cyan-gray volcanic ash, with a porosity of 0.55 under different axial pressures are carried out to analyze the influence of overlying pressure.

Based on the test results demonstrated in **Figure 9**, the soil collapsibility is affected by both water content and axial pressure. The specific manifestation is that the soil collapsibility coefficient is larger under higher axial pressure. In the light of the curved shape, water content corresponding to the highest point of the collapsibility coefficient has an increasing trend with the increase of axial pressure, which is consistent with the changing trend of the optimal water content with axial pressure.

The difference in the apparent phenomena during sample preparation may be an important reason for the different collapsibility of soil. Based on the analysis of the brownish-yellow silty clay with the strongest collapsibility, it is easy to form larger spherical particles under a high water content, and the phenomenon of "conjunctiva" is accompanied with the sieving process. This indicates that the clay content in brownish-yellow silty clay is relatively high, so it is presumed that the clay content is also an important factor affecting collapsibility. The following will verify this presumption through fine particle analysis of three soils.

According to the densitometer method ($d < 0.075$ mm) in Rules of Geotechnical Testing (GB/T50123-2019), the fine particle analysis test was performed on three types of soils.

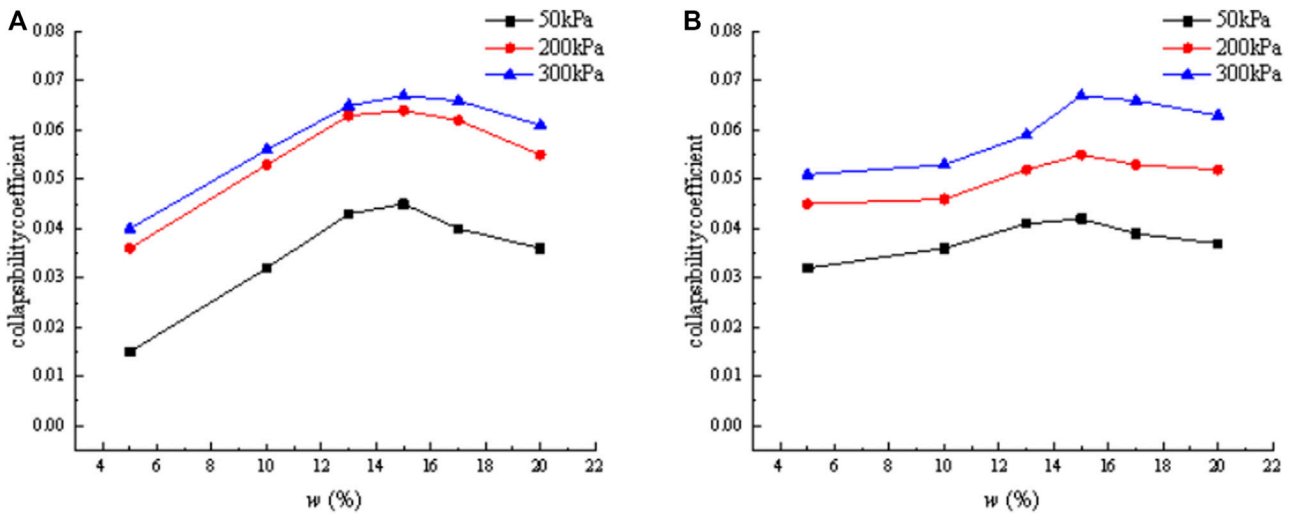

FIGURE 9 | Variation of collapsibility coefficient with water content under different axial pressures. **(A)** Brownish-yellow silty clay; **(B)** cyan-gray volcanic ash.

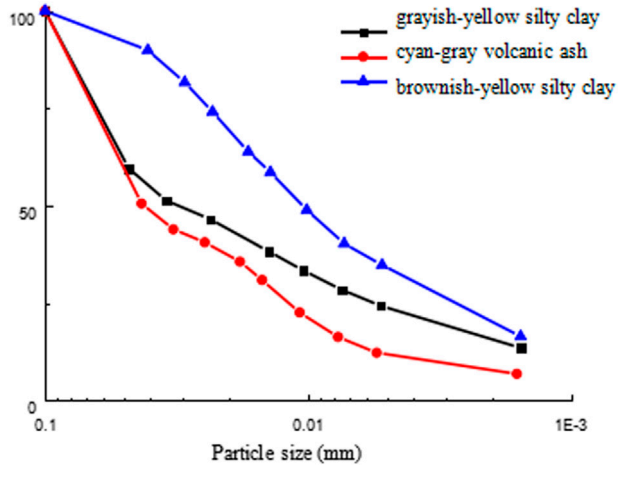

FIGURE 10 | Cumulative curve of finer particle gradation.

The results show that the clay content of grayish-yellow silty clay is 23.96%, and that of brownish-yellow silty clay is 34.81%, which is significantly higher than grayish-yellow silty clay (as represented in **Figure 10**), indicating that the higher the clay content, the stronger the soil collapsibility. But the content of cyan-gray volcanic ash clay is only 12.31%, and its collapsibility is stronger than grayish-yellow silty clay, which indicates that it is unreasonable to evaluate soil collapsibility only by considering the clay content. Combining the phenomena observed in sample preparation, soil collapsibility is analyzed as follows: The effect of clay content on the collapsibility increases with the increasing of clay content, and the clay around skeleton particles will gradually aggregate together. In this process, the fine particles, which were originally scattered in the pores between large particles, will gradually "agglomerate" under the influence of intermolecular attraction and gather towards the large particles. With the further increase of the clay particles' content, the large particles form the "grain chain," and the cohesion increases rapidly. Clay particles begin to play a major role in the macro-mechanical properties, while the "grain chain" completely wraps the large particles and becomes skeleton particles (Shao et al., 2014; Zhang et al., 2015). This phenomenon is especially obvious in soil with low water content and stronger bearing capacity. With the increase of water content, clay particles float, and original skeleton particles are destroyed, resulting in a more obvious settlement than in other similar soils. The soil with stronger binding water capacity forms skeleton particles with better water resistance, which will not be damaged due to the increase of water content and not further settle, that is, soil collapsibility is affected by both clay content and binding water capacity of soil particles (Zhou et al., 2020).

Comprehensive to the above tests and the apparent phenomenon of the cyan-gray volcanic ash after water, the mechanism of collapsibility of the soil can be summarized as follows: for the soil with low clay content, the main cause of collapsibility is the structural damage caused by soaking, such as when water infiltrating into the cyan-gray volcanic ash, its structure of tuff is damaged, and the settlement occurred. For the soil with high clay content, its collapsibility is affected by both clay content and the water-binding capacity of particles. When the binding water capacity of soil particles is strong, the soil will form skeleton particles with good water resistance, which increases the constitutive property of soil and will withhold structural damage due to further soaking. The collapsibility is lower under this state of cyan-gray volcanic ash and gradually decreases until disappears as the water content increases. When the water-binding capacity of soil particles is weak, the soil will form skeleton particles with poor water resistance, and exhibit a certain degree of collapsibility. With the further immersion of the ash, structural damage will occur, the settlement will increase, and exhibit strong collapsibility in general.

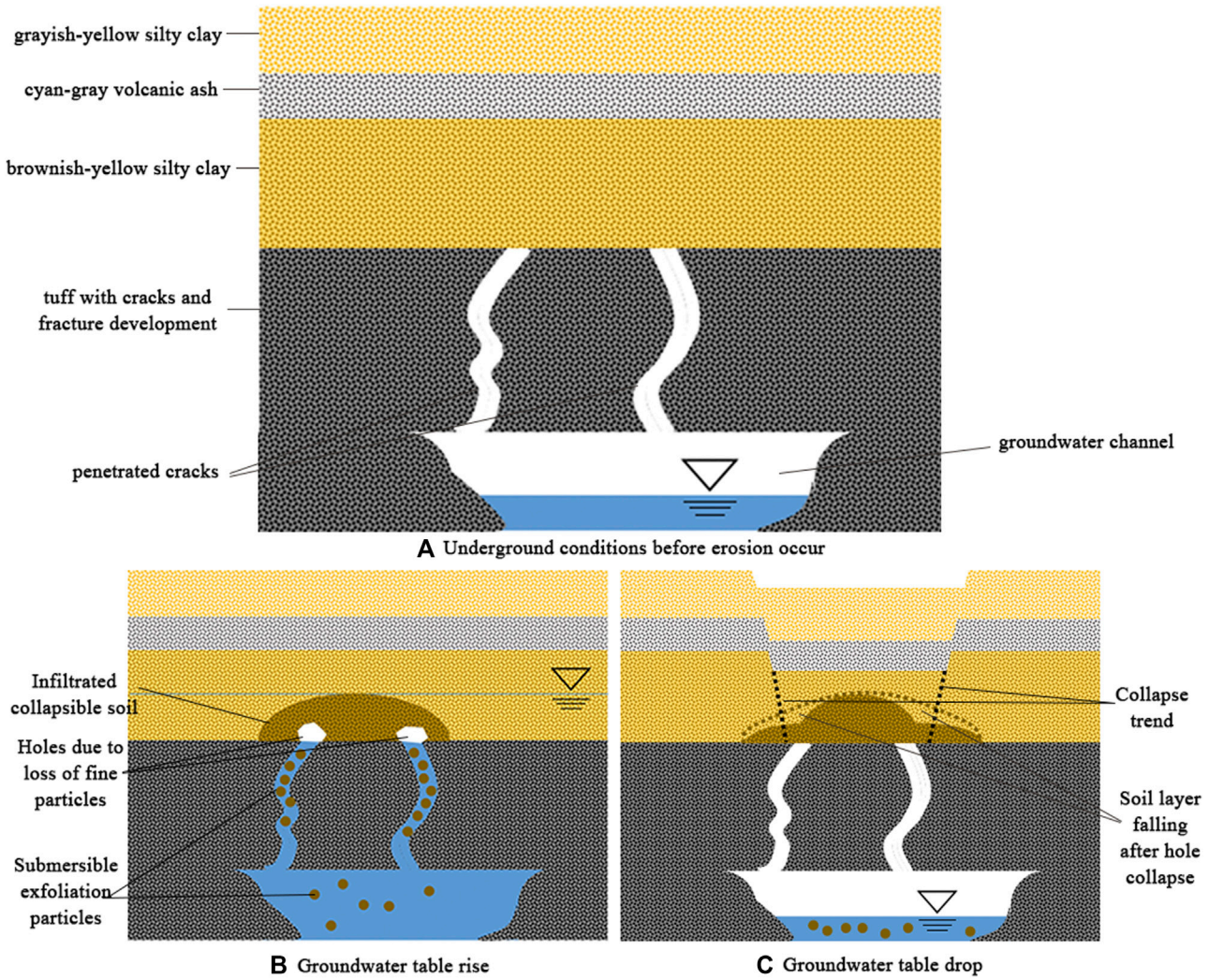

FIGURE 11 | Schematic diagram of the mechanism of surface uneven settlement. **(A)** Underground conditions before erosion occurs; **(B)** groundwater table rise; **(C)** groundwater table drop.

5 DISCUSSION

5.1 Mechanism Analysis of Settlement and Fissure Caused by Soil Collapsibility

Brownish-yellow silty clay with strong collapsibility overlay the bedrock (tuff) with a certain thickness and underlay cyan-gray volcanic ash and grayish-yellow silt clay. With such a soil layer structure, the surface settlement caused by surface water should be even, not localized or belted, whereas what is actually exhibited is the uneven settlement and local fissures. Therefore, it can be considered that the uneven settlement and fissures formed on the surface are not the collapsibility effect caused by surface water. Based on the exploratory trench DK76 results, the location of the surface uneven settlement is directly opposite to the hidden cracks of tuff (**Figure 4B**), which indicates that the uneven settlement is most likely caused by the erosion of groundwater into the overlying soil layer along the hidden cracks, its development process is speculated as follow: When groundwater level rises, water infiltrates into the brownish-yellow silty clay layer through hidden cracks in the bedrock, and the collapsibility causes the fine particles to be stripped from the soil structure and free in the soil layer. When the groundwater level falls, these fine particles are carried out along the bedrock cracks under the action of water flow, causing the soil to be partially lost and the structure of local soil damaged. With the alternating changes of groundwater level height, holes in soil form and gradually develop and penetrate, and the bearing capacity of the brownish-yellow silty clay layer gradually loses, hence ground fissures appear on the surface directly opposite to the hidden cracks, and the overlying soil sink under the further action of groundwater. When the bearing capacity is completely lost due to subsurface erosion, the holes collapse, showing local collapse and

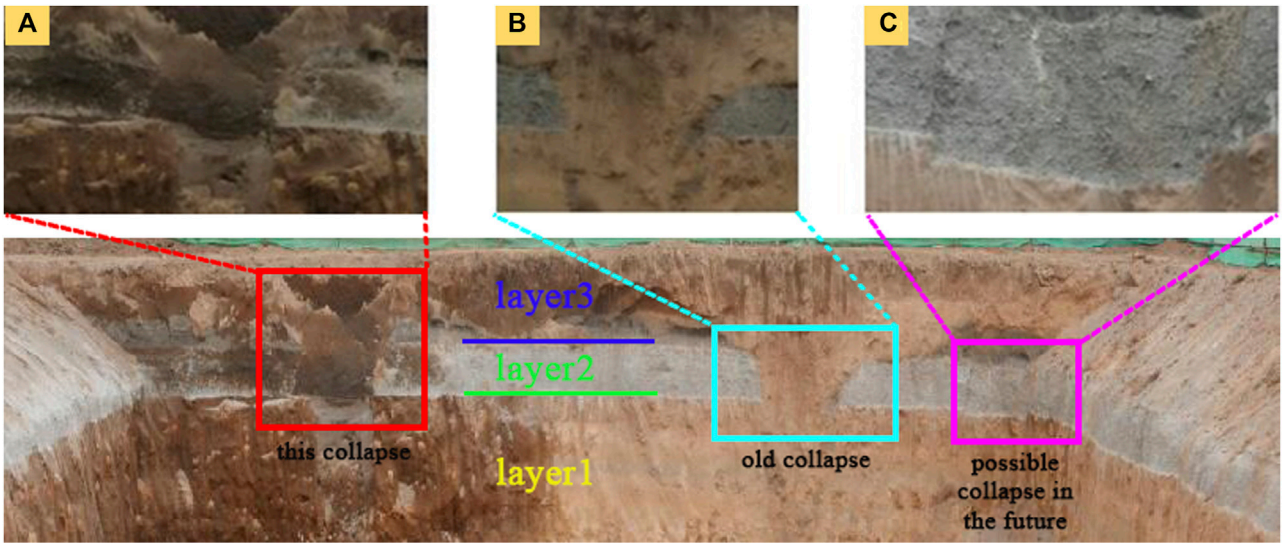

FIGURE 12 | Three collapse positions revealed by the DK76 trench. **(A)** Location of "this collapse"; **(B)** position of "old collapse"; **(C)** position of "possible collapse in the future".

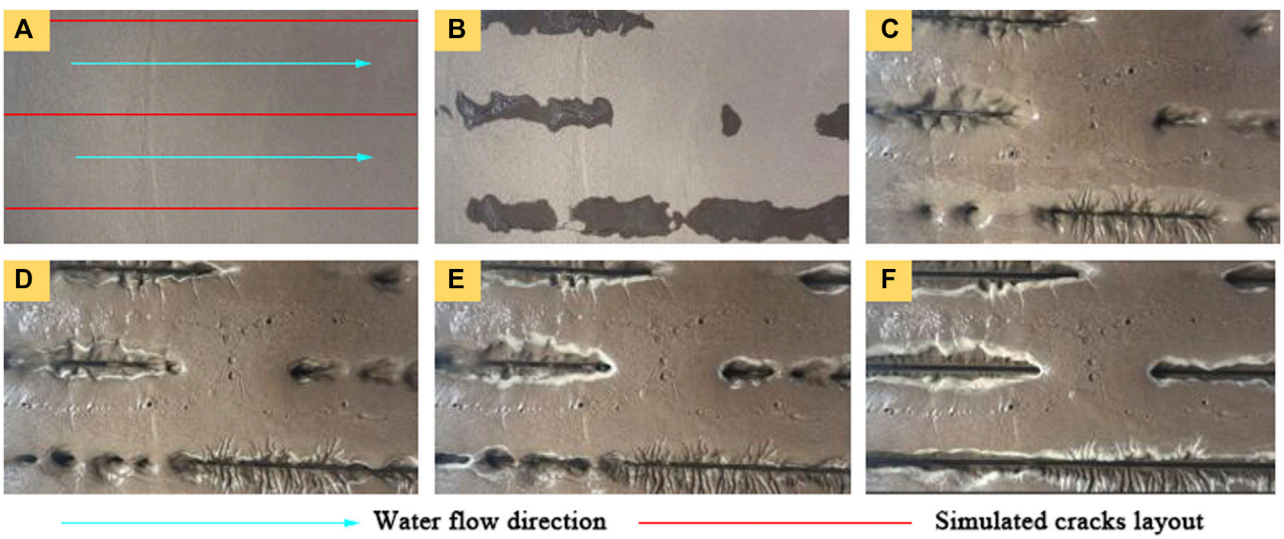

FIGURE 13 | Top view of soil surface collapse before and after soil erosion test. **(A)** After the first water reserve-discharge cycle, **(B)** after three water reserve-discharge cycles; **(C)** after five water reserve-discharge cycles; **(D)** after eight water reserve-discharge cycles; **(E)** after eleven water reserve-discharge cycles; and **(F)** after seventeen water reserve-discharge cycles.

uneven settlement on the surface (the geomorphological phenomenon exhibited in **Figure 2**). A schematic diagram of the mechanism of surface settlement is shown in **Figure 11**.

5.2 Deduce on Influencing Factors of Settlement Degree

As can be seen in **Figure 12**, the volcanic ash layer in the excavated DK76 trench has faults or dislocations at three locations. In "this collapse," it can be seen that the upper part of the volcanic ash layer has collapsed and slid down to the lower part. In "old collapse," we can see that the collapse has occurred before, the soil in the upper part has slipped down to the lower part in the previous collapse, and the collapse did not occur here in this rainfall, probably because the properties of the upper part soil are quite different from the lower part. When the soil adjacent to the bedrock crack is the lower volcanic ash layer, collapse can occur under certain rainfall conditions, while when the soil is in

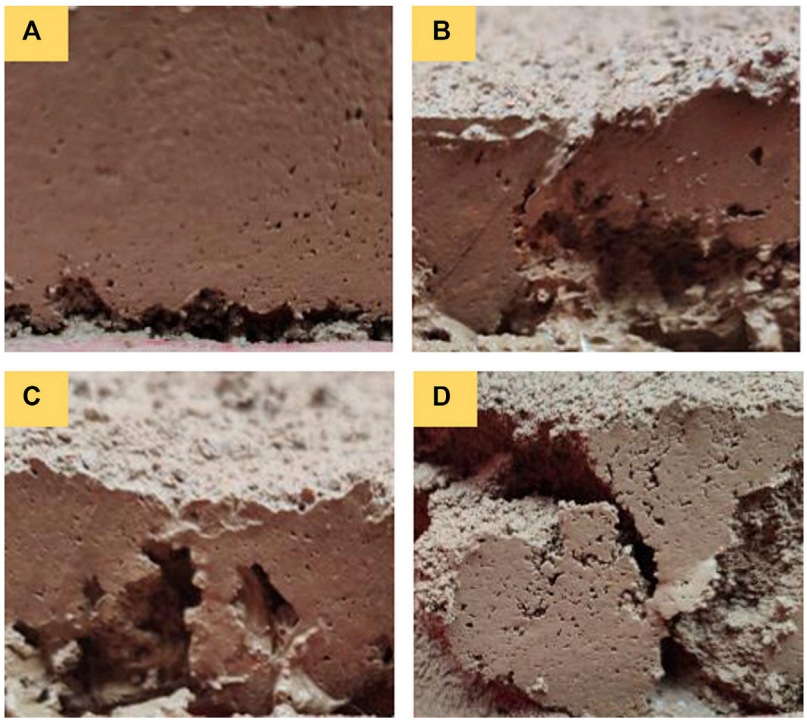

FIGURE 14 | Profile maps of subsurface erosion test. **(A)** Forming small holes; **(B)** the holes expand and penetrate; **(C)** the holes penetrate the soil surface; and **(D)** surface soil collapses.

the upper layer, the collapse will not occur under similar rainfall conditions. At "possible collapse in the future," the volcanic ash layer dislocated, indicating slight collapse has occurred, which may be due to the corresponding bedrock cracks directly below it being relatively narrow or their layouts are not conducive to groundwater erosion, thus leading to a small degree of collapse. In future geological activities or rainfall, the expansion of cracks or the enhancement of groundwater erosion may lead to a new collapse phenomenon at this location.

For the aforementioned inference, our team has set up a series of physical model experiments to verify its rationality. The experimental results show that subsurface erosion can cause the collapse of the overlying soil layer (as shown in **Figure 13**). During the repeated action of groundwater erosion, the change process of the surface soil layer is as follows: first, the soil at the surface layer directly opposite to the simulated cracks becomes wet (**Figure 13A**), next, the whole soil layer is infiltrated (**Figure 13B**), then local holes appear in the surface layer (**Figure 13C**), furthermore the holes penetrate along the simulated cracks (**Figure 13D**), finally the holes further develop and interconnect each other (**Figure 13E**), and a collapse along the simulated cracks is found and the trench is formed (**Figure 13F**). From **Figure 13**, it can qualitatively prove the rationality of the aforementioned inference in this article. The detailed quantitative research results will be published in a subsequent article.

In order to further explain the mechanism of ground fissures, the test profiles are drawn in **Figure 14**. It is seen that the collapse process of collapsibility soil in the subsurface erosion tests from **Figure 14**: under the action of groundwater, first, the collapsible soil layer is hollowed out, forming small holes (**Figure 14A**); next, the holes gradually expand and penetrate with each other under the further action of subsurface erosion (**Figure 14B**); then the holes continue to develop upward and penetrate the soil surface along simulated bedrock cracks (**Figure 14C**); eventually, the surface soil collapses (**Figure 14C**).

Sequential studies will further carry out physical model experiments on loess and silt with similar soil properties to the site soil of the Rift Valley area in Kenya, and quantitative indicators will be used to analyze the influence of collapsibility, hydraulic geology conditions, hidden cracks placement, and other aspects on surface uneven settlement. This article will not reiterate due to the space problem.

6 CONCLUSION

This study analyzes the characteristics and causes of ground fissures and surface uneven settlement in the Rift Valley section of Kenya Nairobi-Malaba Railway, and the main conclusions are as follows:

1) In the context of the regional geology of the Great Rift Valley in East Africa, combined with the field investigations of geological trenching, and drilling, it is found that the surface vegetation is relatively complete at settlement

locations, and holes of varying sizes exist under the surface. The trench excavation shows the left and right bedrock cracks are visible in the weathered layer. The strike of the cracks on the right side of the trench is consistent with surface cracks. The underground cracks are exposed to the overlying soil layer with settlement and collapse, and the discontinuity caused by collapse can be observed in the volcanic ash layer. The crack on the left side is exposed to the new crack position, there is an obvious collapse phenomenon at the overlying soil layer where the bedrock crack is facing directly. The volcanic ash layer is interrupted due to the collapse; thus, it is related to the bedrock crack.

2) Analysis of factors affecting collapsibility shows that the larger the axial pressure, the stronger the collapsibility of soil, and the higher the water content corresponding to the extreme value of collapsibility coefficient. In addition, taking into account the apparent phenomena during the sample preparation, the collapsibility mechanism of various types of soil is discussed from the perspectives of clay content and water-binding capacity of soil particles, for cyan-gray volcanic ash, the main cause of collapsibility is the structural damage caused by soil encountering water; for grayish-yellow silty clay, as its particles have the strong water-binding capacity and form skeleton particles with good water resistance after water, the soil collapsibility is weak after the soil is completely infiltrated; for brownish-yellow silty clay, the skeleton particles formed by water have poor water resistance due to their weak water binding capacity and exhibit strong collapsibility after the soil is fully saturated.
3) Soil collapsibility and groundwater erosion are the important causes of ground fissures and uneven surface settlement; this study infers that the causes of ground cracks in the Rift Valley are related to the settlement of overlying soil and the loss of soil particles. In the process of groundwater infiltration and outflow along bedrock cracks, the soil layer is affected by collapsibility and eroding at the same time, manifesting as a small amount of local settlement and loss of certain bearing capacity accompanied by structural damage. Meanwhile, soil particles are continuously lost along bedrock cracks, forming holes, further developing and penetrating. When the holes develop to a certain scale, the overlying soil loses its bearing capacity, and a hole first appears on the surface. As the holes continuously developed and penetrated, further instability and collapse form uneven settlement and ground fissures. During the rainy season, it is scoured by surface rainwater and then develops into gullies or ditches. Subsequently, the author will analyze the influence of groundwater erosion on ground fissures and uneven surface settlement through further experiments.

DATA AVAILABILITY STATEMENT

The original contributions presented in the study are included in the article/**Supplementary Material**, further inquiries can be directed to the corresponding author.

AUTHOR CONTRIBUTIONS

XL provided the background conditions for the research. ZZ contributed to the conception of the study and the materials needed for the experiments. designed and completed the series of experimental works. BH and YL processed and analyzed the results. BH wrote the first draft of the manuscript. YL enriched the manuscript and improved the quality of all the images. ZZ revised and embellished the language, and LJ revised the overall framework and format of the manuscript. All authors read and approved the submitted version.

ACKNOWLEDGMENTS

The author is grateful for the financial support for the study presented in this article from the National Natural Science Foundation of China (Grant Nos U1839202 and U2039208).

SUPPLEMENTARY MATERIAL

The Supplementary Material for this article can be found online at: https://www.frontiersin.org/articles/10.3389/feart.2022.909102/full#supplementary-material

REFERENCES

Ayalew, L., Yamagishi, H., and Reik, G. (2004). Ground Cracks in Ethiopian Rift Valley: Facts and Uncertainties. *Eng. Geol.* 75 (3–4), 309–324. doi:10.1016/j.enggeo.2004.06.018

Budhu, M. (2011). Earth Fissure Formation from the Mechanics of Groundwater Pumping. *Int. J. Geomech.* 11, 1–11. doi:10.1061/(asce)gm.1943-5622.0000060

Conway, B. D. (2015). Land Subsidence and Earth Fissures in South-Central and Southern Arizona, USA. *Hydrogeol. J.* 24 (3), 649–655. doi:10.1007/s10040-015-1329-z

Elahe, J., Philip, J., Vardon, S. C., and Steele, D. (2020). The Impact of Evaporation Induced Cracks and Precipitation on Temporal Slope Stability. *Comput. Geotechnics* 122, 103506. doi:10.1016/j.compgeo.2020.103506

Feng, D., Hou, E. K., Xie, X. S., and Che, X. Y. (2022). Prediction and Treatment of Water Leakage Risk Caused by the Dynamic Evolution of Ground Fissures in Gully Terrain. *Front. Earth Sci.* 3, 1–12. doi:10.3389/feart.2021.803721

Fergason, K. C., Rucker, M. L., and Panda, B. B. (2015). Methods for Monitoring Land Subsidence and Earth Fissures in the Western USA. *Proc. IAHS* 372, 361–366. doi:10.5194/piahs-372-361-2015

Gabrielli, C. P., Mcdonnell, J. J., and Jarvis, W. T. (2011). The Role of Bedrock Groundwater in Rainfall-Runoff Response at Hillslope and Catchment Scales. *J. Hydrol.* 450-451 (15), 117–133. doi:10.1016/j.jhydrol.2012.05.023

Howard, K. W. F., and Zhou, W. (2019). Overview of Ground Fissure Research in China. *Environ. Earth Sci.* 78 (3), 97. doi:10.1007/s12665-019-8114-6

Jia, Z., Lu, Q., Peng, J., Qiao, J., Wang, F., Wang, S., et al. (2020). Analysis and Comparison of Two Types of Ground Fissures in Dali County in the Weihe Basin, China. *Environ. Earth Sci.* 79 (1), 38. doi:10.1007/s12665-019-8783-1

Jin, W.-z., Luo, Z.-j., and Wu, X.-h. (2016). Sensitivity Analysis of Related Parameters in Simulation of Land Subsidence and Ground Fissures Caused

by Groundwater Exploitation. *Bull. Eng. Geol. Environ.* 75 (3), 1143–1156. doi:10.1007/s10064-016-0897-z

Leng, X. L., Wang, C., Zhang, J., Sheng, Q., Cao, S. L., and Chen, J. (2021). Deformation Development Mechanism in a Loess Slope with Seepage Fissures Subjected to Rainfall and Traffic Load. *Front. Earth Sci.* 9, 769257. doi:10.3389/feart.2021.769257

Leonard, R. J. (1929). An Earth Fissure in Southern Arizona. *J. Geol.* 37, 765–774. doi:10.1086/623676

Liu, H., Deng, K., Lei, S., and Bian, Z. (2015). Mechanism of Formation of Sliding Ground Fissure in Loess Hilly Areas Caused by Underground Mining. *Int. J. Min. Sci. Technol.* 25 (4), 553–558. doi:10.1016/j.ijmst.2015.05.006

Liu, N., Feng, X., Huang, Q., Fan, W., Peng, J., Lu, Q., et al. (2019). Dynamic Characteristics of a Ground Fissure Site. *Eng. Geol.* 248, 220–229. doi:10.1016/j.enggeo.2018.12.003

Nina, L., Xiao, F., Huang, Q. B., Wen, F., Peng, J. B., and Lu, Q. Z. (2019). Dynamic Characteristics of a Ground Fissure Site. *Eng. Geol.* 248, 220–229. doi:10.1016/j.enggeo.2018.12.003

Peng, J., Sun, X., Lu, Q., Meng, L., He, H., Qiao, J., et al. (2020). Characteristics and Mechanisms for Origin of Earth Fissures in Fenwei Basin, China. *Eng. Geol.* 266, 105445. doi:10.1016/j.enggeo.2019.105445

Sarkar, I. (2004). The Role of the 1999 Chamoli Earthquake in the Formation of Ground Cracks. *J. Asian Earth Sci.* 22 (5), 529–538. doi:10.1016/s1367-9120(03)00093-2

Shao, S. J., Wang, L. Q., Hu, T., and Wang, Q. (2014). Structural Index of Loess and its Relation with Granularity, Density and Humidity. *J. Geotechnical Eng.* 36 (8), 1387–1393. doi:10.11779/CJGE201408002

Timothy, G. C., Jung, H. K., George, P. M., Jae, K. K., Benedikt, H., and Apostolos, S. P. (2016). Effects of Tectonic Regime and Soil Conditions on the Pulse Period of Near-Fault Ground Motions. *Soil Dyn. Earthq. Eng.* 80, 102–118. doi:10.1016/j.soildyn.2015.09.011

Wadge, G., Biggs, J., Lloyd, R., and Kendall, J. M. (2016). Historical Volcanism and the State of Stress in the East African Rift System. *Front. Earth Sci.* 4, 86. doi:10.3389/feart.2016.00086

Wang, D. W., Liu, D., and Zhou, Z. G. (2019). Ground Fissure Characteristics of Great Rift Valley in Kenya and Railway Construction Countermeasure, China. *Subgr. Eng.* 4, 233–239. doi:10.13379/j.issn.1003-8825.2019.04.46

Wang, F., Peng, J., Chen, Z., Wang, Q., Meng, Z., Qiao, J., et al. (2020). Development Characteristics and Mechanisms of Damage-Causing Urban Ground Fissures in Datong City, China. *Eng. Geol.* 271, 105605. doi:10.1016/j.enggeo.2020.105605

Xu, L., Li, S., Cao, X., Somerville, I. D., Suo, Y., Liu, X., et al. (2016). Holocene Intracontinental Deformation of the Northern North China Plain: Evidence of Tectonic Ground Fissures. *J. Asian Earth Sci.* 119 (1), 49–64. doi:10.1016/j.jseaes.2016.01.003

Youssef, A. M. (2013). Overview of Some Geological Hazards in the Saudi Arabia. *Environ. Earth Sci.* 70 (31), 15–30. doi:10.1007/s12665-013-2373-4

Youssef, A. M., Sabtan, A. A., Maerz, N. H., and Zabramawi, Y. A. (2014). Earth Fissures in Wadi Najran, Kingdom of Saudi Arabia. *Nat. Hazards.* 71 (3), 2013–2027. doi:10.1007/s11069-013-0991-5

Zhang, J. R., Hu, Y., Yu, H. L., and Tao, G. L. (2015). Predicting Soil-Water Characteristic Curve from Multi-Fractal Particle-Size Distribution of Clay. *J. Hydraulic Eng.* 46 (6), 650–657. doi:10.13243/j.cnki.slxb.20141323

Zhou, X. X., Chi, S. C., Jia, Y. F., and Shao, X. Q. (2020). A New Wetting Deformation Simulation Method Based on Changes in Mechanical Properties. *Comput. Geotechnics* 117, 10326. doi:10.1016/j.compgeo.2019.103261

Conflict of Interest: The authors declare that the research was conducted in the absence of any commercial or financial relationships that could be construed as a potential conflict of interest.

Publisher's Note: All claims expressed in this article are solely those of the authors and do not necessarily represent those of their affiliated organizations, or those of the publisher, the editors, and the reviewers. Any product that may be evaluated in this article, or claim that may be made by its manufacturer, is not guaranteed or endorsed by the publisher.